Supporting Information

Visible-light active nanohybrid TiO_2/carbon photocatalysts with programmed morphology by direct carbonization of block copolymer templates

Saji Thomas Kochuveedu,[a] Yu Jin Jang,[a] Yoon Hee Jang,[a] Won Jun Lee,[b] Min-Ah Cha,[a] Haeyoung Shin,[c] Seokhyun Yoon,[c] Sang Soo Lee,[d] Sangouk Kim,[b] Kwanwoo Shin,[e] Martin Steinhart*[f] and Dong Ha Kim*[a]

[a]*Department of Chemistry and Nano Science, Division of Molecular and Life Sciences, College of Natural Sciences, Ewha Womans University, 52, Ewhayeodae-gil, Seodaemun-gu, Seoul, 120-750, Korea*

[b]*Department of Material Science and Engineering, Korea Advanced Institute of Science and Technology, Daejon, Korea.*

[c]*Department of Nanosciences/Physics, Ewha Womans University, 11-1 Daehyun-dong, Seodaemun-gu, Seoul, 120-750, Korea*

[d]*Polymer Hybrid Research Center, Korea Institute of Science and Technology, P.O Bpx 131, Cheongryang, Seoul 130-650, Korea.*

[e]*Department of Chemistry Interdisciplinary Program of Integrated Biotechnology, Sogang University, Seoul, Korea.*

[f]*Institute for Chemistry, University of Osnabrueck, Osnabrueck, Germany.*

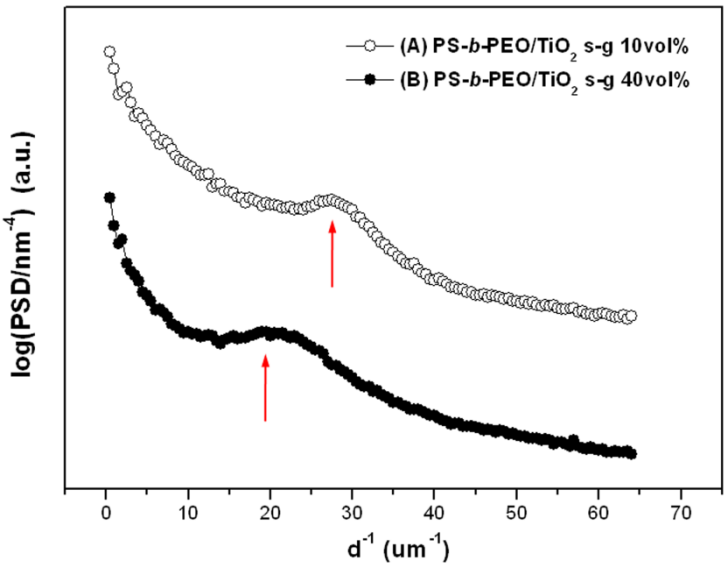

Fig. S1 Power spectral density profiles obtained from the AFM images displayed in Figure 2A and B of as-cast TiO_2/PS-*b*-PEO films obtained with (A) 10 vol-% and (B) 40 vol-% TiO_2 sol-gel precursor solution. The spectra were vertically shifted.

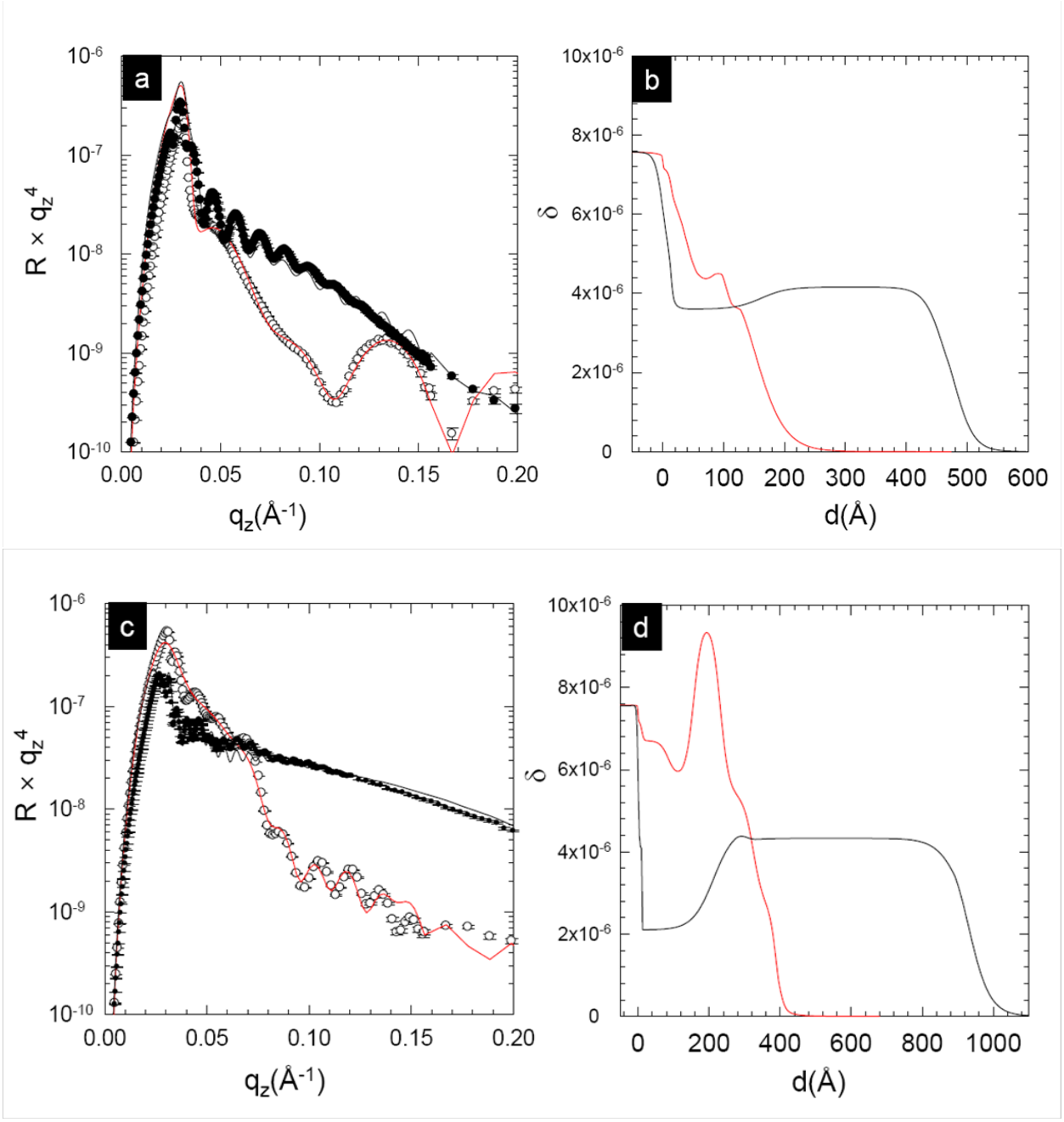

Fig. S2 X-ray reflectivity of (a) the as-cast TiO_2/PS-*b*-PEO films obtained with 10 vol-% TiO_2 precursor solution (closed circles) and the corresponding C-TiO_2 films obtained after carbonization (open circles). Lines represent the best fit obtained from (b) the corresponding dispersion profiles (black line: as-cast, red line: after carbonization). X-ray reflectivity of (c) the as-cast TiO_2/PS-*b*-PEO films obtained with 40 vol-% TiO_2 sol-gel precursor solution (closed circles) and the corresponding C-TiO_2 films obtained after carbonization (open circles). Lines represent the best fit obtained from (d) the corresponding dispersion profiles (black line: as-cast, red line: after carbonization).

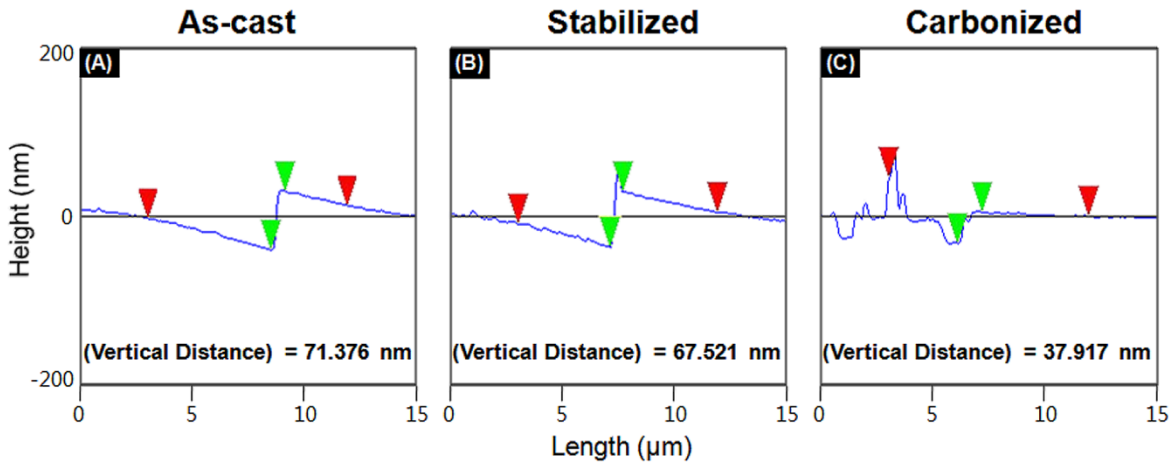

Fig. S3 Step height analysis of (A) as-cast, (B) stabilized, and (C) carbonized films obtained with 40 vol-% TiO_2 precursor solution that were scratched with a razor blade. The red markers represent the scan length, whereas the position of the steps is indicated by the green markers.

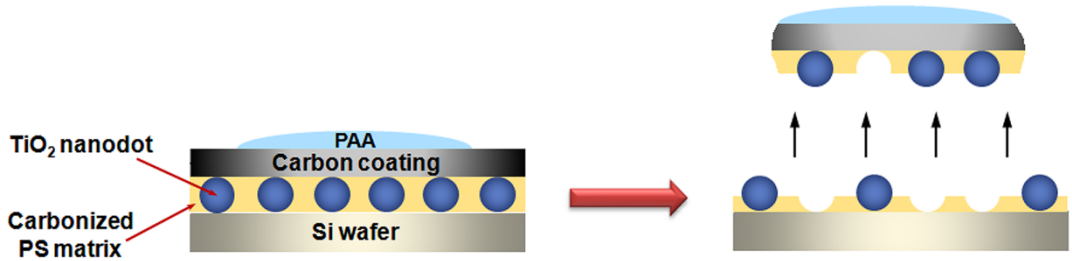

Fig. S4 Schematic illustration of the preparation of TEM specimens. During the detachment of TiO_2/carbon-carbon-PAA multilayer from the Si wafer, the TiO_2/carbon hybrid films were partially damaged. The detached carbonized hybrid films containing TiO_2 nanodots were then floated on a water surface and transferred to TEM grids.

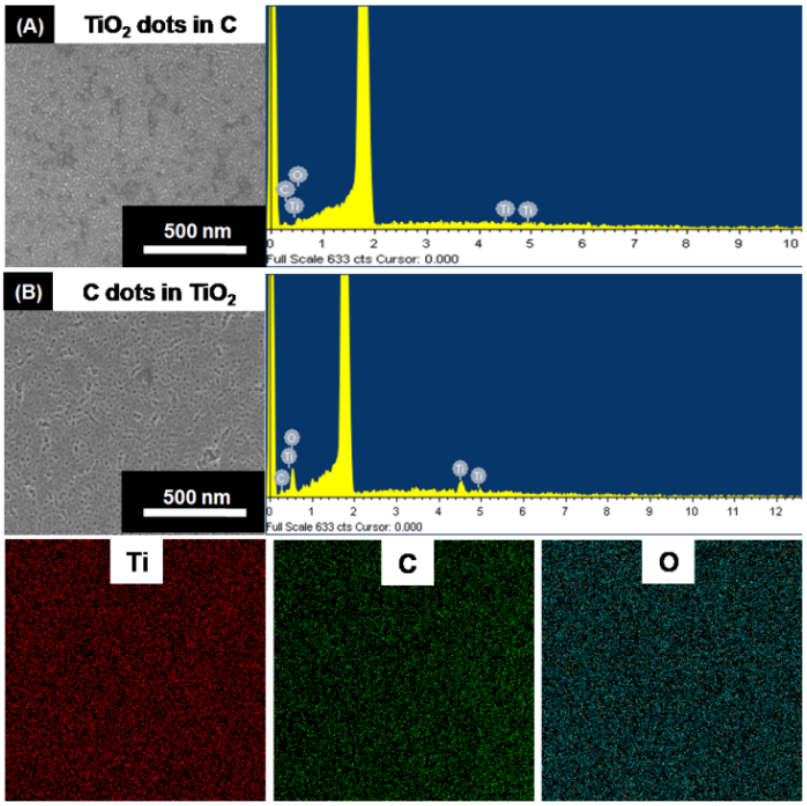

Fig. S5 SEM images and EDS of TiO_2 dots in C matrix (A); C dots in TiO_2 matrix (B) and its corresponding elemental mapping.

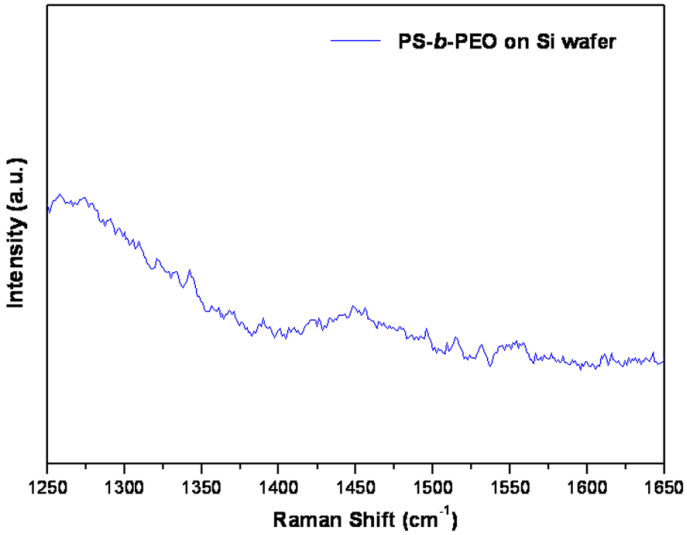

Fig. S6 Raman spectrum of a silicon wafer coated with a pure PS-*b*-PEO thin film before carbonization.

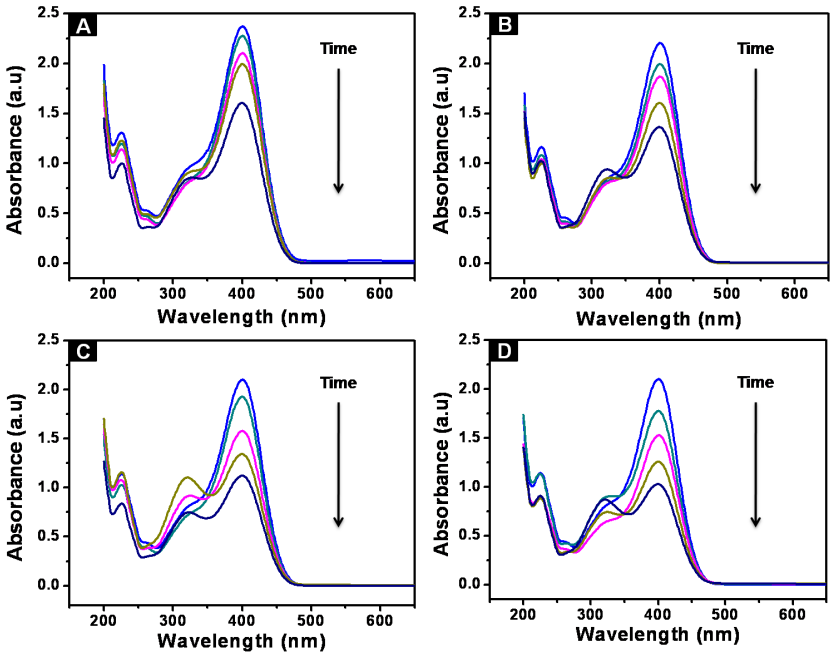

Fig. S7 Visible-light photocatalytic activitiy of C-TiO_2 hybrid nanostructures in the degradation of *p*-nitrophenol. The initial height of the absorbance maximum at around ~400 nm in the absorbance spectrum of *p*-nitrophenol prior to irradiation with UV light was used as a reference. Successive decrease of the peak height was assumed to correspond to the relative decrease in *p*-nitrophenol concentration. (A) TiO_2 dots in C nanostructure in a film; (B) C dots in TiO_2 nanostructure in a film; (C) TiO_2 dots in C nanostructure in powder form; (D) C dots in TiO_2 nanostructure in powder form.

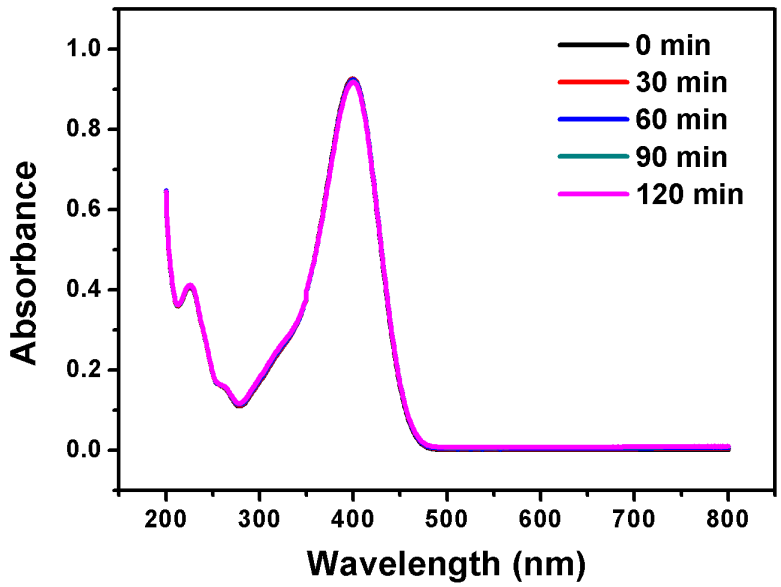

Fig. S8 Absorption spectrum of a pure aqueous solution containing 10 ppm *p*-nitrophenol in the absence of catalyst used as a reference for the evaluation of the photocatalytic efficiency of C-TiO_2 systems in the degradation of *p*-nitrophenol.